IBDW2014-00103-F0033
ASSOCIATION OF THE g.27563G > A OSTEOPROTEGERIN GENETIC POLYMORPHISM WITH BONE MINERAL DENSITY IN CHINESE WOMEN

Y. P. Liu, D. W. Zhao, W. M. Wang, B. J. Wang, Y. Zhang, Z. G. Li
The Affiliated Zhongshan Hospital of Dalian University, PR China

Introduction and aims: Osteoporosis is a common multifactorial disease in postmenopausal women. This study aimed to investigate the association between the g.27563G>A osteoprotegerin (OPG) genetic polymorphism and bone mineral density (BMD) and osteoporosis.
Methods: A case-control study was carried out in 435 osteoporotic postmenopausal women and 442 age-matched healthy controls. The BMD at the femoral neck, lumbar spine (L2-4) and total hip was assessed by Norland XR-46 dual-energy X-ray absorptiometry. The genotypes of the g.27563G>A genetic polymorphism were detected by created restriction site-polymerase chain reaction and verified by DNA sequencing methods.
Results: We detected that the g.27563G>A genetic polymorphism was a non-synonymous mutation that resulted in an arginine (Arg) to glutamine (Gln) amino acid replacement (p.Arg333Gln). Significant differences were found in the BMD of the femoral neck, lumbar spine (L2-4) and total hip and different genotypes of the g.27563G>A genetic polymorphism. Subjects with the genotype GG had significantly higher BMD values than those with genotypes GA and AA ($P < 0.05$).
Conclusion: Our data indicated that the A allele of the g.27563G>A genetic polymorphism in OPG could be associated with lower BMD values in Chinese postmenopausal women and that it might be a risk factor for osteoporosis.

IBDW2014-00104-F0034
ASSESSMENT OF JOINT LYMPHATIC DRAINAGE FUNCTION USING INDOCYANINE GREEN NEAR-INFRARED IMAGING IN OVINE

Qianqian Liang, Ph.D [a,b], Yan Chen, Ph.D. [a,b], Yongjian Zhao, M.D. [a,b], Ronald W. Wood, Ph.D. [e], Chenguang Li, Ph.D. [a,b], Jixiang Shi, M.D.,Ph.D. [f], Jinlong Li, M.D. [a,b], Lianping Xing, Ph.D. [c,d,e], Yongjun Wang, Ph.D. [a,b]
[a]*Department of Orthopaedics, Longhua Hospital, Shanghai University of Traditional Chinese Medicine, Shanghai 200032, China*
[b]*Institute of Spine, Shanghai University of Traditional Chinese Medicine, Shanghai 200032,China*
[c]*Department of Pathology and Laboratory Medicine, University of Rochester Medical Center,601 Elmwood Avenue, Rochester, NY 14642, USA*
[d]*Center for Musculoskeletal Research, University of Rochester Medical Center, 601 ElmwoodAvenue, Rochester, NY 14642, USA*
[e]*Department of Obstetrics and Gynecology, Urology, and Neurobiology and Anatomy,University of Rochester Medical Center, 601 Elmwood Avenue, Rochester, NY 14642, USA*
[f]*Department of Orthopaedics, Putuo Hospital, Shanghai University of Traditional Chinese Medicine, Shanghai 200062, China*

Introduction and aims: To assess the peri-articular lymphatic function at knee and ankle joints of normal ovine using an Indocyanine Green Near-Infrared (ICG-NIR) Imaging system
Methods: ICG was injected into the ankle and knee joints of two normal ovine, the hind legs were illuminated with a 780-nm NIR laser to record the movement of ICG dye from the joints to the upstream regional lymph nodes. The trafficking and clearance of ICG and lymphatic pulses were assessed. When the animals were euthanized, their lymphatic vessels and lymph nodes were dissected under NIR guidance after intra-joint injection of ICG and Evans blue dye. The location of lymphatic vessels that drained ICG was examined.
Results: ICG-NIR detected two lymphatic vessels efferent from the ankle joints toward the popliteal lymph nodes and lymphatic pulses. After ICG was injected directly into the joint synovial space, the ICG signal accumulated at the site of injection, peaked at 24hours and decreased thereafter. At 72 hours, more than 90% of injected ICG was disappeared from the joint. The optimal exposure time for NIR laser is around 50ms to 100ms. Lymphatic vessels efferent from the knee joint were embedded in soft fat tissues and hardly detected by NIR without dissection.
Conclusion: Our findings suggest that ICG-NIR can be used to assess the lymphatic draining function in ovine joints, which provides critical information for its potential use in joints of patients with arthritis.

IBDW2014-00105-F0035
DIFFUSION TENSOR IMAGING FOR ANATOMICAL AND QUANTITATIVE EVALUATION OF THE ANTERIOR CRUCIATE LIGAMENT GRAFTS

Xianfeng Yang [a], Dongyang Chen [b], Dongquan Shi [b], Bin Zhu [a], Qing Jiang [b]
[a]*Department of Radiology, the Affiliated Drum Tower Hospital of Nanjing University Medical School, China*
[b]*Department of Orthopaedics Surgery, the Affiliated Drum Tower Hospital of Nanjing University Medical School, China*

Introduction and aims: To explore the feasibility and repeatability of diffusion tensor imaging (DTI) and diffusion tractography (DTT) on the anterior cruciate ligament graft after reconstruction and determine the fractional anisotropy (FA) and apparent diffusion coefficient (ADC) values.
Methods: Twenty-two patients with ACL reconstruction operation were scanned by 3T clinical MR scanner. The fiber tracking and other post-processing steps were carried out twice by a radiologist on the workstation and repeated by another radiologist. Diffusion tensor metrics of different parts of the grafts were determined with region of interest (ROI)- and fiber tractography (FT)-based measurements and the intra- and inter-observer measurement variance were calculated.
Results: Tractography illustrated nicely the 3D courses of the graft in all 22 cases. The mean FA value of the intra-tunnel part was significantly higher than that of the intra-articular part, whereas the mean ADC value of the intra-tunnel part was lower than that of the intra-articular part. According to two-sided paired samples Student's *t* test, the intra- and inter-observer measurements correlated well.
Conclusion: DTI and DTT can be used to visualize the ACL grafts and can provide additional information over standard morphologic MR imaging.

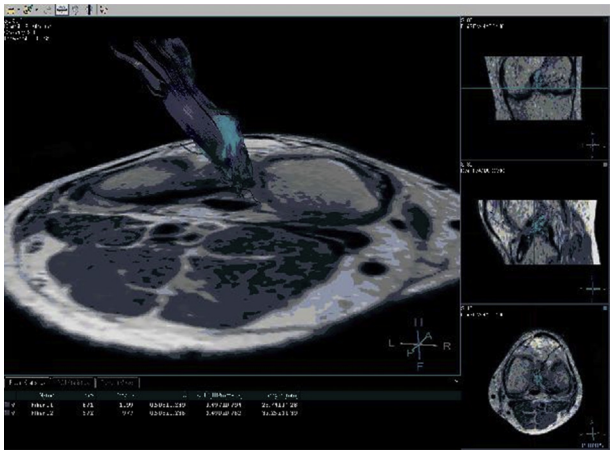

IBDW2014-00106-F0036
PHYTOESTROGENIC MOLECULE ICARITIN PREVENTS OVX-INDUCED OSTEOPOROSIS IN MICE

Jing Long [a,b], Qiufeng Zhou [a,b], Dan Li [a], Xinluan Wang [a], Huijuan Cao [a], Ling Qin [a,c]
[a]*Translational Medicine Research and Development Center, Shenzhen Institutes of Advanced Technology, Chinese Academy of Sciences, Shenzhen 518055, China*
[b]*Institute of Biotechnology, Guilin Medical University, Guilin 541004, China*
[c]*Department of Orthopaedics and Traumatology, The Chinese University of Hong Kong*

Introduction and aims: The objective of this study was to evaluate the effect of the early icaritin treatment on uterus, trabecular microarchitecture and bone biomechanics in adult ovariectomized (OVX) mice.
Methods: Thirty 3-month-old female mice were sham-operated (Sham, n = 10) or ovariectomized (n = 20). Ten OVX mice were subjected to icaritin treatment (ICT, 160mg/kg/d) at 3 days after operation, and the vehicle-treated Sham and OVX mice served as corresponding controls. Both icaritin and vehicle treatment lasted for 10 weeks. The uterus indexes were measured and the trabecular architecture and biomechanical properties of the 5th lumbar vertebrae were analyzed with micro-CT and mechanical

testing, respectively. The uteruses and decalcified femurs were then embedded in paraffin and sectioned for histopathological examination.
Results: Compared with the Sham group, the uterus indexes reduced significantly in OVX and ICT mice, with no significant difference between OVX and ICT mice. Histopathological examination of uterus showed a thinned endometrium with atrophic glands in OVX and ICT mice. Micro-CT analysis showed that the bone mineral density, bone volume/tissue volume, trabecular number and trabecular thickness of the 5th lumbar vertebrae all decreased significantly, and the trabecular separation increased in OVX mice. Mechanical testing showed that the biomechanical properties of the 5th lumbar vertebrae in OVX mice reduced, including the sectional elastic modulus, the maximum failure force and the energy absorbed until failure. Histopathological examination of femurs showed thin and spaced trabecular bone accompanied by increased bone marrow fat content in OVX mice. However, these osteoporotic phenotypes were rescued in ICT mice.
Conclusion: Icaritin can prevent OVX-induced osteoporosis in mice, without hyperplastic effect on uterus.
Acknowledgements
This work was supported by the grants from NSFC (No. 81200650 and 81302782).

IBDW2014-00107-F0037
INVESTIGATION OF HIERARCHICAL POROUS MICROSTRUCTURE OF SHANKBONE

B. Chen, D. Yin, S. Lin
College of Aerospace Engineering, Chongqing University, Chongqing 400044, China

Introduction and aims: Bone possesses high fracture strength and toughness. Simultaneously, it is also relatively light. The excellent mechanical and physical properties of the bone are highly related to its elaborate microstructure refined by nature over many centuries. The detailed research on bone microstructure and the relationship between the microstructure and the properties of the bone can reveal the mechanism of strength and toughness as well as light-weight of the bone.
Methods: In this study, the hierarchical porous microstructure of a shankbone was first analyzed by a scanning electron microscope (SEM) under different scales and directions. Then an image processing with a higher gray-scale resolution was used to analyze the SEM images of the porous microstructure of the bone under different scales. The porosity at different locations of the bone under different directions was identified. Lastly, the number and size of pores and density of the bone along different directions and under different scales were investigated by a MATLAB program.
Results: It was revealed that the bone was a porous bioceramics composite with particularly porous microstructure which varied by different scales, location and direction. It was indicated that the number and size of pores and density of the bone varied with the observed locations, directions and scales.
Conclusion: The polynomial expressions for the number and size of the pore and density of the bone are fitted from the relation curves between the number and size of the pores and density of the bone and the locations, directions and scales, which reveals the hierarchical porous microstructural characteristic of the bone.

IBDW2014-00108-F0038
RELATIONSHIP BETWEEN MICROSTRUCTURE AND MECHANICAL BEHAVIOR OF CORTICAL BONE

B. Chen, S. Lin, D. Yin
College of Aerospace Engineering, Chongqing University, Chongqing 400044, China

Introduction and aims: The mechanical behaviors of the bone, such as fracture susceptibility, are closely related to the microstructure of the bone. Therefore, the investigation on the relationship between the mechanical behavior and the microstructure of the bone is important. This investigation used the experiment and models of microscopic mechanics. The combination of the experiment and analytical models at microscopic scale could provide a fair understanding of the mechanical behavior of the bone.
Methods: In this work, the observation of scanning electron microscope, nanoindentation technique, hierarchical-model analysis and finite element computation at microscopic scale were used to investigate the relationship between the mechanical behavior of a cortical bone and its microstructure, such as its porosity, density and the direction of the hydroxyapatite-fiber sheets. In the hierarchical-model analysis, the osteons in the cortical bone were first considered as hollow fibers and the interstitial bone as matrix, and then the osteons were further taken as a combination of many hydroxyapatite-fiber plies. Each fiber ply had different direction and modulus that provided different contributions to the mechanical properties of the bone. The porosity in the bone as well as the direction of the hydroxyapatite-fiber sheets in the osteons were modeled explicitly based on the images of the scanning electron microscope and X-ray diffraction. Computational results were obtained by applying uniform macroscopic stress to the boundaries of the microscopic model of the bone.
Results: The prediction of the macroscopic mechanical property corresponded reasonably well with the experimental data.
Conclusion: The relationship between the mechanical behavior and the microstructure of the bone is discussed in detail.

IBDW2014-00109-F0039
TISSUE MINERAL DENSITY DEPENDENT MECHANICAL PROPERTIES OF INDIVIDUAL TRABECULA PLATES AND RODS DO NOT DIFFER IN ANATOMIC DIRECTIONS BUT INDIVIDUAL TRABECULAR DIRECTIONS

Yue Eric Yu, Ji Wang, Bin Zhou, X. Edward Guo
Department of Biomedical Engineering, Columbia University, NY, USA

Introduction and aims: Trabecular bone, susceptible to osteoporosis, consists of individual trabecular plates and rods, which are distributed distinctly along the longitudinal, transverse, or oblique anatomic directions of the skeleton (Fig.1). In each anatomic direction, mechanical properties of bone tissue are also expected to differ in (axial) or against (lateral) the direction of individual trabeculae, i.e., anisotropic mechanical properties. However, anisotropic mechanical properties of individual trabeculae along various anatomic directions are currently unclear. **Objectives** of this study were 1) to measure anisotropic tissue modulus and tissue mineral density (TMD) of individual trabeculae; 2) to examine their dependence on trabecular types and anatomic directions; and 3) to determine the relationship between anisotropic tissue modulus and TMD of individual trabeculae.
Methods: Twelve cylindrical human trabecular bone samples of proximal femurs were imaged with hydroxyapatite density calibration phantoms at 25μm resolution by micro-computed tomography (μCT). Individual trabecular types and their anatomic directions were determined using individual trabeculae segmentation (ITS) technique. On the embedded samples, microindentation tests were performed under wet condition on both axial and lateral cross-sections (Fig 1.C) of selected plates and rods in longitudinal (L), transverse (T), and oblique (O) directions, respectively (Fig 1.D). The point-by-point registered grayscale values of the μCT image at the indentation sites were converted to TMD using calibration phantoms.
Results: The tissue modulus and the co-localized TMD of trabecular plates were significantly higher than those of trabecular rods (Fig. 2A, B). The axial tissue modulus of individual trabeculae was significantly higher than the lateral tissue modulus (Fig. 2C). The tissue modulus correlated strongly with TMD. These correlations did not differ significantly between plates and rods or between different anatomic directions. However, the correlation of axial modulus was significantly different from that of lateral modulus (Fig. 2D).
Conclusion: We measured anisotropic elastic modulus of individual trabecular plates and rods of different anatomic directions. Surprisingly, the heterogeneous tissue modulus correlated with TMD similarly regardless of trabecular types and anatomic directions. The correlation only differs

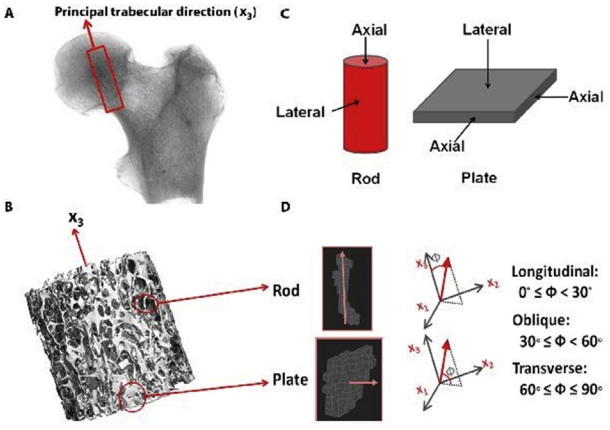

A. X-ray radiography illustration of the principle trabecular direction of femoral neck trabecular bone
B. μCT illustration of the trabecular structure of a cylinder sample corresponding to the red box in Fig.1 A
C. Axial and lateral directions of trabecular plates and rods
D. Classification of anatomic directions of plates and rods